

**IMECE2003-41571**

## MELTING AND RESOLIDIFICATION OF A TWO-COMPONENT METAL POWDER LAYER HEATED BY A MOVING GAUSSIAN HEAT SOURCE

Tiebing Chen and Yuwen Zhang  
Department of Mechanical and  
Aerospace Engineering  
University of Missouri-Columbia  
Columbia, MO 65211  
zhangyu@missouri.edu

### ABSTRACT

Melting and resolidification of a subcooled mixed metal powder layer that contains a mixture of two metal powders with significantly different melting points heated by a moving Gaussian heat source is investigated numerically. The phase change is modeled using a temperature-transforming model and shrinkage induced by melting is also taken into account. The problem appears to be steady-state since it is formulated in a coordinate system moving with the Gaussian heat source and the size of the powder is much larger than that of the heat source. The results show that the powder layer thickness, moving heat source intensity and scanning velocity have significant effects on the sintering depth.

### NOMENCLATURE

$b$	moving heat source half width ( $m$ )	$k$	thermal conductivity ( $W / m K$ )
$B_i$	Biot number, $hb / k_H$	$K$	dimensionless thermal conductivity, $k / k_H$
$C$	dimensionless heat capacity, $C^0 / C_H^0$	$N_i$	dimensionless moving heat source intensity, $\alpha_a I_0 b / [k_H (T_m^0 - T_i^0)]$
$C^0$	heat capacity, $\rho c_p$	$N_R$	radiation number, $\varepsilon_e \sigma (T_m^0 - T_i^0)^3 b / k_H$
$c_p$	specific heat, ( $W / kg \text{ } ^\circ C$ )	$N_t$	temperature ratio for radiation, $T_m^0 / (T_m^0 - T_i^0)$
$e$	enthalpy, $J / kg$	$q$	strength of line heat source ( $W / m$ )
$E$	dimensionless enthalpy, $e / C_H^0 (T_m^0 - T_i^0)$	$s$	solid-liquid interface location ( $m$ )
$h$	convective heat transfer coefficient ( $W / m^2 K$ )	$s_0$	location of surface ( $m$ )
$h_m$	latent heat of melting or solidification, $J / kg$	$s_{st}$	sintered depth ( $m$ )
$I_0$	center heat source intensity ( $W / m^2$ )	$Sc$	subcooling parameter, $C_H^0 (T_m^0 - T_i^0) / (\rho_L h_{sl})$
		$T$	dimensionless temperature, $(T^0 - T_m^0) / (T_m^0 - T_i^0)$
		$t$	false time (s)
		$T^0$	temperature ( $^\circ C$ )
		$u$	heat source moving velocity ( $m / s$ )
		$U$	dimensionless heat source moving velocity, $ub / \alpha_H$
		$V$	volume ( $m^3$ )
		$w$	velocity of liquid phase ( $m / s$ )
		$W$	dimensionless velocity of the liquid phase, $wb / \alpha_H$
		$x$	moving horizontal coordinate
		$X$	dimensionless moving horizontal coordinate, $x / b$
		$z$	vertical coordinate ( $m$ )
		$Z$	dimensionless vertical coordinate, $z / b$

## Greek symbol

$\alpha$	thermal diffusivity ( $m^2 / s$ )
$\alpha_a$	absorbivity
$\delta$	powder layer thickness, m
$\Delta$	dimensionless powder layer thickness, $\delta / b$
$\Delta T^0$	one-half of phase-change temperature range ( $K$ )
$\Delta T$	one-half of dimensionless phase change temperature range
$\varepsilon$	volume fraction of gas (porosity for unsintered powder), $V_g / (V_g + V_L + V_H)$
$\varepsilon_e$	emissivity of surface
$\eta$	dimensionless solid-liquid interface location, $s / b$
$\eta_0$	dimensionless location of the surface, $s_0 / b$
$\eta_{st}$	dimensionless sintered depth, $s_{st} / b$
$\rho$	density ( $kg / m^3$ )
$\sigma$	Stefan-Boltzman constant, $5.67 \times 10^{-8} W / (m^2 K^4)$
$\tau$	false dimensionless time, $\alpha_H t / b^2$
$\phi$	volume percentage of low melting point powder, $V_L / (V_L + V_H)$

## Subscripts

$eff$	effective
$H$	high melting point powder
$L$	low melting point powder
$m$	melting point
$p$	sintered parts
$s$	solid

## 1. INTRODUCTION

Selective Laser Sintering (SLS), which can rapidly fabricate functional parts from CAD design, is an emerging technology of Solid Freeform Fabrication (SFF) [1]. In SLS of metal powder, near full density objects are fabricated due to rapid solidification immediately after melting induced by scanning of laser beam. Since melting and resolidification are the mechanism of laser-based solid freeform fabrication of metals, inclusion of melting and solidification in the model of SLS is essential.

Fundamentals of melting and solidification have been investigated extensively in the literatures [2, 3]. Laser-induced melting of the metal powder is different from the normal melting since the significant density change occurs in the process due to the shrinkage. The single-component powder system is used in the early research but it is unsuccessful because of the “balling” phenomena [4]. In order to avoid “balling” phenomena, the powder mixture composed of two types of powders possessing significantly different melting points was suggested by Bunnell [5] and Manzur *et al.* [6]. It

should be noted that only the low-melting-point powder melts and resolidifies in SLS. Zhang and Faghri analytically solved the one-dimensional melting of a semi-infinite two-component metal powder bed heated by the constant heat flux [7]. Since the thickness of consecutive powder layers is very small (0.1 – 0.25 mm) in SLS, melting of metal powders actually occurs in a very thin layer. Chen and Zhang [8] obtained the analytical solution of one-dimensional melting of the two-component metal powder bed with finite thickness subjected to constant heat flux heating, which is an approximation of SLS of the first layer of the metal powder.

For two-dimensional modeling, a numerical simulation of the melting and resolidification of subcooled semi-infinite two-component metal powder bed with a moving Gaussian heat source was presented by Zhang and Faghri [9]. The thickness of the computational domains used in Ref. [9] was very large, which is again a good approximation of the first layer of SLS but is not accurate for the consecutive layers. In order to simulate SLS of the consecutive layers, it is necessary to investigate melting/solidification of a two-component metal powder layer with finite thickness. In this paper, the effects of the powder layer thickness, moving heat source intensity and scanning velocity on the formation of the liquid pool and the sintering depth in a two-dimensional metal powder layer will be investigated numerically.

## 2. PHYSICAL MODEL

The physical model of the melting and resolidification problem of the two-component metal powder layer is shown in Fig. 1. The powder layer, which is infinite horizontally but finite vertically, is subjected to a moving Gaussian heat source and its bottom is adiabatic. The initial temperature of the powder layer is below the melting point of the low-melting-point powder and then melting does not occur immediately until the top surface temperature of the powder layer reaches the melting point of the low-melting-point powder. After melting starts, the liquid pool is formed when the powders interact with the moving Gaussian heat source and then resolidified when the heat source moves away. Melting of the powder layer always accompanies the significant density change due to the shrinkage since the high-melting-powder particle alone can not sustain the powder structure. This shrinkage phenomenon induced by melting is desirable since fully densified part can be formed from the loose metal powder particles.

Since the size of the heat source, which has an order of magnitude of  $10^{-3}$  m, is very small compared from the size of the powder layer in horizontal direction, the quasi-steady-state is obtained. A moving coordinate system of which the origin is fixed at the center of heat source is employed [9]. The dimensionless energy equation for the physical problem is

$$-U \frac{\partial E}{\partial X} + W \frac{\partial E}{\partial Z} = \frac{\partial}{\partial X} \left( K \frac{\partial T}{\partial X} \right) + \frac{\partial}{\partial Z} \left( K \frac{\partial T}{\partial Z} \right) \quad (1)$$

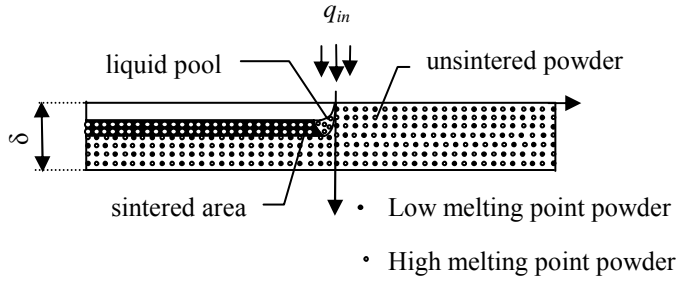


Fig. 1 Physical Model

where the dimensionless variables are defined in the nomenclature. The thermal properties of the two-component metal powder bed can be found in Ref. [9].

The temperature transforming model [10] is employed in order to convert the enthalpy-based energy equation into a temperature-based energy equation. In this methodology, the solid-liquid phase change is assumed to occur in a range of phase-change temperatures from  $T_m^0 - \Delta T^0$  to  $T_m^0 - \Delta T$ . It can also be successfully used to simulate the melting and solidification which occur at a specific temperature by assuming the very small  $\Delta T$ . Based on the temperature transforming model, the relation between enthalpy and temperature can be expressed as

$$E = \begin{cases} (1-\epsilon)(\phi C_L + 1 - \phi)T & T < -\Delta T \\ [(1-\epsilon)(\phi C_L + 1 - \phi) + (1-\epsilon)\phi \frac{C_L}{2Sc\Delta T}]T + \frac{(1-\epsilon)\phi C_L}{2Sc} & -\Delta T < T < \Delta T \\ (1-\epsilon)(\phi C_L + 1 - \phi)T + \frac{(1-\epsilon)\phi C_L}{2Sc} & T > \Delta T \end{cases} \quad (2)$$

A temperature function is introduced, i.e.,  $E = CT + S$ , and eq. (1) becomes

$$-U \frac{\partial(CT)}{\partial X} + W \frac{\partial(CT)}{\partial Z} = \frac{\partial}{\partial X} \left( K \frac{\partial T}{\partial X} \right) + \frac{\partial}{\partial Z} \left( K \frac{\partial T}{\partial Z} \right) - (-U \frac{\partial S}{\partial X} + W \frac{\partial S}{\partial Z}) \quad (3)$$

The dimensionless vertical velocity,  $W$ , in the liquid pool induced by shrinkage is

$$W = \begin{cases} -\epsilon_s U \frac{\partial \eta_{st}}{\partial X} & Z \leq \eta_{st} \\ 0 & Z > \eta_{st} \end{cases} \quad (4)$$

In arrival to eq. (4), it is assumed that the volume fraction of the gas in the sintered region is zero and fully densified part layer is obtained [8]. The dimensionless heat capacity,  $C$ , and the source term,  $S$ , and The dimensionless thermal conductivity,  $K$ , are

$$C = \begin{cases} (1-\epsilon)(\phi C_L + 1 - \phi) & T < -\Delta T \\ (1-\epsilon)(\phi C_L + 1 - \phi) + (1-\epsilon)\phi \frac{C_L}{2Sc\Delta T} & -\Delta T < T < \Delta T \\ (1-\epsilon)(\phi C_L + 1 - \phi) & T > \Delta T \end{cases} \quad (5)$$

$$S = \begin{cases} 0 & T < -\Delta T \\ \frac{(1-\epsilon)\phi C_L}{2Sc} & -\Delta T < T < \Delta T \\ \frac{(1-\epsilon)\phi C_L}{Sc} & T > \Delta T \end{cases} \quad (6)$$

$$K = \begin{cases} K_{eff} & T < -\Delta T \\ K_{eff} + \frac{K_p - K_{eff}}{2\Delta T} (T + \Delta T) & -\Delta T < T < \Delta T \\ K_p & T > \Delta T \end{cases} \quad (7)$$

The corresponding boundary conditions of eq. (3) are as following

$$-K \frac{\partial T}{\partial Z} = N_i \exp(-X^2) - N_r [(T + N_i)^4 - (T_\infty + N_i)^4] - B_i (T - T_\infty), \quad Z = \eta_0(X) \quad (8)$$

$$\frac{\partial T}{\partial Z} = 0, \quad Z = \Delta, \quad -\infty \leq X \leq \infty \quad (9)$$

$$T = -1, \quad |X| \rightarrow \infty, \quad 0 \leq Z \leq \Delta \quad (10)$$

With the assumption that the sintered part is fully densified, the location of the surface is related to the sintered depth by

$$\eta_0(X) = \epsilon_s \eta_{st}(X) \quad (11)$$

### 3. NUMERICAL SOLUTION

The melting and resolidification problem that was formulated in the preceding section is a steady-state problem in the moving coordinate system. A false transient method is employed and the converged steady-state solution is declared when the temperature distribution and locations of the liquid-solid interface and liquid surface do not vary with the false time. The finite volume method [11] is employed to discretise the eq. (3) with additional false transient term, of which the conduction-convection terms are interpreted by the power-law scheme [11]. The computational domain has an irregular shape which is composed of unsintered powder, liquid pool and sintered region as shown in the physical model due to the shrinkage. A block-off technique [11] is employed so that the computational domain is rectangular shape. The thermal conductivity in the empty space created by the shrinkage is zero.

In order to obtain the quasi-steady-state, the computational domain in  $X$  direction must be large enough compared with the dimension of moving heat source. The computation was carried

out for a non-uniform grid in X direction and uniform grid in Z direction. The dimensionless length of computational domain in X direction is 40 and the dimensionless thickness in Z direction varies from 0.25 to 1.0. The grids of  $122 \times (27 \sim 52)$  are used depending on the thickness of metal powder layer. The dimensionless false time step used in the numerical solution is  $\Delta\tau = 10^{-4}$ . Finer grids and smaller time steps were also used in the simulation but no noticeable difference is found. Based on the temperature transforming model, a very small dimensionless phase-change temperature range,  $\Delta T = 0.001$ , is chosen in the simulation in order to simulate melting and solidification occurred at a single temperature.

#### 4. RESULTS AND DISCUSSIONS

The thickness of the mixed metal powder layer, dimensionless moving heat source intensity, and dimensionless moving heat source velocity are dominant processing parameters of the SLS process since all of them have significant effects on melting and resolidification. Figure 2 shows the effect of the dimensionless moving heat source intensity on the sintering process for  $\Delta = 0.25$ . As can be seen, the sintering depth increases significantly with increasing heat source intensity and the entire liquid pool moves slightly toward the positive X direction at the same time. When the heat source intensity is lower, the liquid pool appears to be an irregular shape that has a large volume in the upper part and suddenly turns to be much slim downward. The upper part of the liquid pool stretches in the opposite direction of the moving heat source like a tail. When the sintering depth reaches the bottom surface of powder layer, the liquid pool turns to be full and the tail of the liquid pool is vanished.

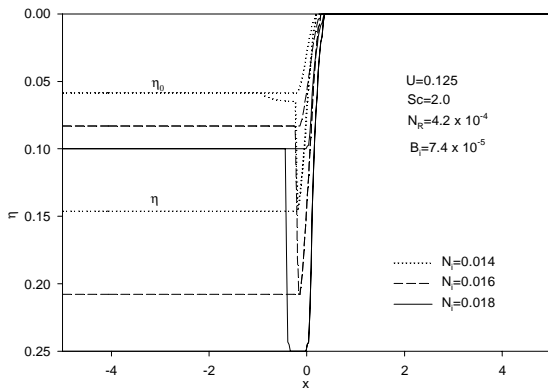


Fig. 2 Effect of the heat source intensity on the sintering process when  $\Delta = 0.25$

Figure 3 shows the effect of the scanning velocity on the sintering process for  $\Delta = 0.25$ . It can be observed that the sintering depth decreases with the increasing scanning velocity, which is due to the fact that the interaction between the moving heat source and powder layer is shortened when the heat source

moves fast. The whole liquid pool moves slightly toward the opposite direction of the heat source motion when the scanning velocity increases.

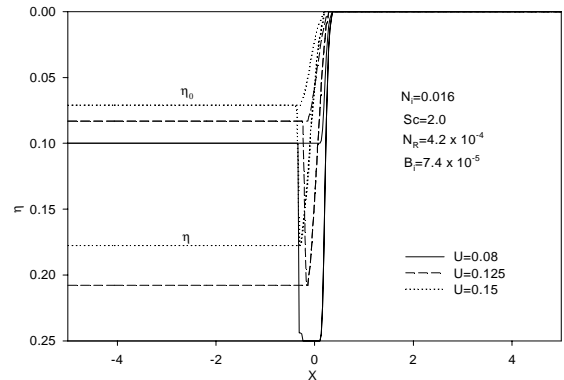


Fig. 3 Effect of scanning velocity on the sintering process when  $\Delta = 0.25$

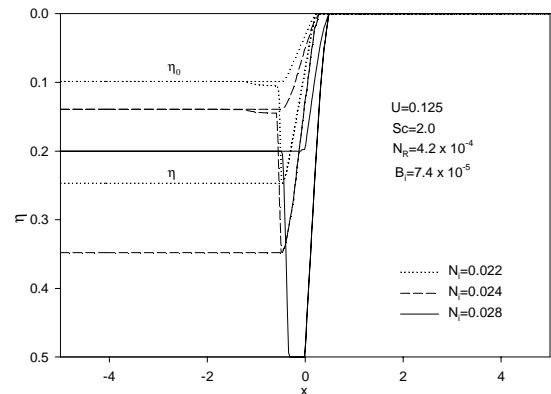


Fig. 4 Effect of the heat source intensity on the sintering process when  $\Delta = 0.50$

Figure 4 shows the effect of the dimensionless moving heat source intensity on the sintering process for  $\Delta = 0.50$ . It is also apparent that the sintering depth increases accompanied with the increase of dimensionless moving heat source intensity. The liquid pool also moves slightly toward the opposite direction of the heat source motion with the increasing heat source intensity. The tail of the liquid pool is also occurred. Compared with the case in Fig. 2, the larger heat source intensity is needed in order to melt the powder layer under the same scanning velocity since more heat is conducted into the loose powder for the thicker powder layer. The effect of the scanning velocity on the sintering process for  $\Delta = 0.50$  is shown in Fig. 5. It can also be observed that the sintering depth decreases when the scanning velocity is decreased from 0.125 to 0.15. The shape of the liquid pool has the similar trend of change compared with that in Fig. 3. The effect of the dimensionless moving heat source

intensity on the sintering process for  $\Delta = 1.0$  is shown in Fig. 6. Figure 7 shows the effect of the scanning velocity on the sintering process for  $\Delta = 1.0$ . The similar phenomena found in Fig. 2- 5 can also be observed.

$$N_i = \begin{cases} 0.0284 U^{0.2308}, & \Delta = 0.25 \\ 0.0323 U^{0.0857}, & \Delta = 0.50 \\ 0.0506 U^{0.0792}, & \Delta = 1.00 \end{cases} \quad (12)$$

where  $U > 0$ . The parameters used in the simulation are shown in Table 1.

Table 1 Processing parameters used in simulation of empirical correlation

$Sc$	2.0	$N_t$	1.5
$N_R$	$4.2 \times 10^{-4}$	$T_\infty$	-1.0
$B_i$	$7.4 \times 10^{-5}$	$U$	0.075 ~ 0.175
$\Delta_s$	0.25, 0.5, 1.0	$\phi$	0.4
$K_{LH}$	2.9	$C_{LH}$	0.7
$\mathcal{E}_s$	0.4		

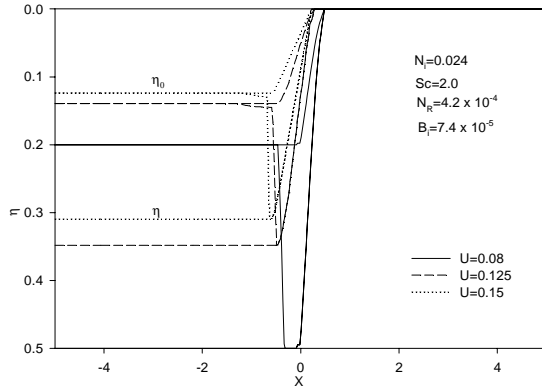


Fig. 5 Effect of scanning velocity on the sintering process when  $\Delta = 0.50$

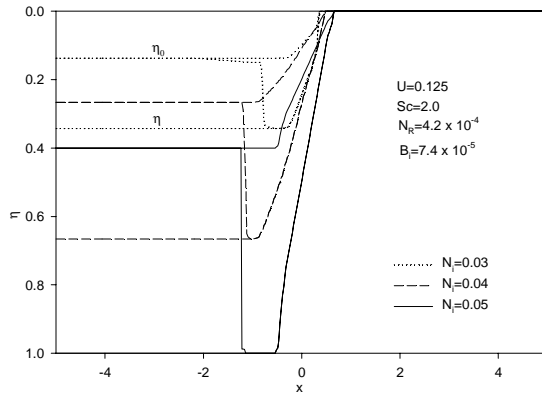


Fig. 6 Effect of the heat source intensity on the sintering process when  $\Delta = 1.0$

In an ideal process, it is desirable to use optimized processing parameters so that the entire powder layer can be molten and resolidified. A parametric study is performed to obtain the optimized dimensionless moving heat source intensity at the specific scanning velocity for the different thickness of powder layer. The dimensionless moving heat source intensity is varied in the optimization process and the optimized dimensionless moving heat source intensity is obtained when the sintering depth reaches the bottom of powder layer. Figure 8 shows the optimized dimensionless moving heat source intensity plotted as a function of scanning velocity,  $U$ , for different thickness of powder layer which is 0.25, 0.5, and 1.0 respectively. The empirical correlation is as following:

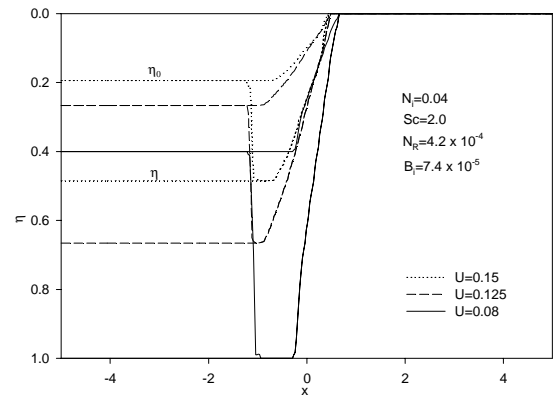


Fig. 7 Effect of scanning velocity on the sintering process when  $\Delta = 1.0$

## 5. CONCLUSION

Melting and resolidification of a two-dimensional metal powder layer with a very thin thickness heated by a moving heat flux was investigated numerically. The results indicate that the sintering depth increases with the increasing moving heat source intensity or decreasing scanning velocity. The larger moving heat source intensity is needed to achieve the same sintering depth at a specific scanning velocity when the thickness of powder layer is increased. An empirical correlation on the optimized dimensionless moving heat source intensity is obtained.

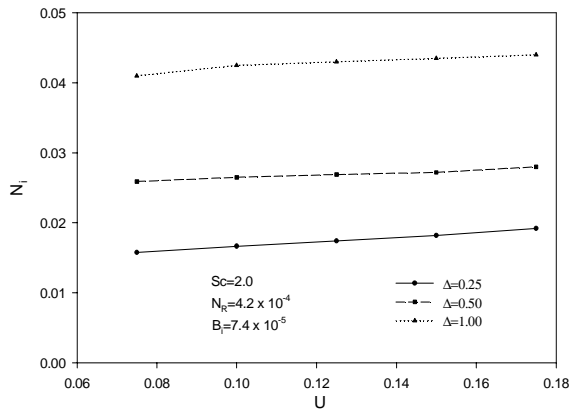


Fig. 8 Optimized dimensionless heat source intensity at different scanning velocity

Moving Gaussian Heat Source,” *ASME Journal of Heat Transfer*, **120**, pp 883-891.

[10] Cao, Y., and Faghri, A., 1990, “A numerical analysis of phase change problems including natural convection,” *Journal of Heat Transfer* **112**, pp 812-816.

[11] Patankar, S. V., 1980, *Numerical Heat Transfer and Fluid Flow*, McGraw-Hill, New York.

## ACKNOWLEDGMENTS

Support for this work by the Office of Naval Research under the grant number N00014-02-1-0356 is greatly acknowledged.

## REFERENCES

- [1] Conley, J. G., and Marcus, H.L., 1997, “Rapid Prototyping and Solid Freeform Fabrication,” *Journal of Manufacturing Science and Engineering*, **119**, pp 811-816.
- [2] Viskanta, R., 1983, Phase change heat transfer, in: G.A. Lane (Ed.), *Solar Heat Storage: Latent Heat Materials*, CRC Press, Boca Raton, FL.
- [3] Yao, L. C., and Prusa, J., 1989, “Melting and freezing,” *Advances in Heat Transfer*, **25**, pp1-96.
- [4] Bourell, D.L., Marcus, H.L., Barlow, J.W., and Beaman, J.J., 1992, “Selective laser sintering of metals and ceramics,” *International Journal of Powder Metallurgy*, **28**, No.4, pp. 369-81.
- [5] Bunnell, D.E., 1995, *Fundamentals of selective laser sintering of metals*, Ph.D. Thesis, University of Texas at Austin.
- [6] Manzur, T., DeMaria, T., Chen, W., and Roychoudhuri, C., 1996, “Potential Role of High Powder Laser Diode in Manufacturing,” presented at SPIE Photonics West Conference, San Jose, CA.
- [7] Zhang, Y., and Faghri, A., 1999, “Melting of a Subcooled Mixed powder Bed with Constant Heat Flux Heating,” *International Journal of Heat and Mass Transfer*, **42**, pp. 775-788.
- [8] Chen, T., and Zhang, Y., 2003, “Analysis of Melting in a Mixed Powder Bed with Finite Thickness Subjected to Constant Heat Flux Heating,” *Proceeding of ASME Summer Heat Transfer Conference*, Las Vegas, NV.
- [9] Zhang, Y., and Faghri, A., 1998, “Melting and Resolidification of a Subcooled Mixed Powder Bed with